

Longitudinal CSF proteome profiling in mice to uncover the acute and sustained mechanisms of action of rapid acting antidepressant (2R,6R)-hydroxynorketamine (HNK)

David P. Herzog^{a,*}, Natarajan Perumal^{b,1}, Caroline Manicam^b, Giulia Treccani^{a,c,d}, Jens Nadig^a, Milena Rossmann^b, Jan Engelmann^a, Tanja Jene^a, Annika Hasch^a, Michael A. van der Kooij^{a,e}, Klaus Lieb^{a,e}, Nils C. Gassen^f, Franz H. Grus^b, Marianne B. Müller^{a,e,**}

^a Department of Psychiatry and Psychotherapy and Focus Program Translational Neurosciences, Johannes Gutenberg University Medical Center Mainz, Mainz, Germany

^b Experimental and Translational Ophthalmology, Department of Ophthalmology, Johannes Gutenberg University Medical Center, Mainz, Germany

^c Institute for Microscopic Anatomy and Neurobiology, Johannes Gutenberg University Medical Center, Mainz, Germany

^d Translational Neuropsychiatry Unit, Department of Clinical Medicine, Aarhus University, Risskov, Denmark

^e Leibniz Institute for Resilience Research, Mainz, Germany

^f Neurohomeostasis Research Group, Department of Psychiatry and Psychotherapy, University Medical Center Bonn, Bonn, Germany

ARTICLE INFO

Keywords:

Antidepressant
CSF
Ketamine
(2R,6R)-Hydroxynorketamine
Proteomics
Glucocorticoid receptor signaling

ABSTRACT

Delayed onset of antidepressant action is a shortcoming in depression treatment. Ketamine and its metabolite (2R,6R)-hydroxynorketamine (HNK) have emerged as promising rapid-acting antidepressants. However, their mechanism of action remains unknown. In this study, we first described the anxious and depression-prone inbred mouse strain, DBA/2J, as an animal model to assess the antidepressant-like effects of ketamine and HNK *in vivo*. To decode the molecular mechanisms mediating HNK's rapid antidepressant effects, a longitudinal cerebrospinal fluid (CSF) proteome profiling of its acute and sustained effects was conducted using an unbiased, hypothesis-free mass spectrometry-based proteomics approach. A total of 387 proteins were identified, with a major implication of significantly differentially expressed proteins in the glucocorticoid receptor (GR) signaling pathway, providing evidence for a link between HNK and regulation of the stress hormone system. Mechanistically, we identified HNK to repress GR-mediated transcription and reduce hormonal sensitivity of GR *in vitro*. In addition, mammalian target of rapamycin (mTOR) and brain-derived neurotrophic factor (BDNF) were predicted to be important upstream regulators of HNK treatment. Our results contribute to precise understanding of the temporal dynamics and molecular targets underlying HNK's rapid antidepressant-like effects, which can be used as a benchmark for improved treatment strategies for depression in future.

1. Introduction

A well-recognized shortcoming of currently available pharmacological agents in the treatment of major depressive disorder (MDD) is that significant difference from placebo can only be reliably identified 4–6 weeks after treatment onset (Johnston et al., 2019). This therapeutic

delay of classical antidepressants is potentially dangerous since suicide risk is the highest in the early treatment period when the disease severity is at its greatest (Dong et al., 2019). The absence of rapid positive feedback also encourages non-compliance, thus increasing duration of the depressive episode and the overall costs for treating this disease (Sobocki et al., 2006). In addition, the lack of biomarkers for disease

* Corresponding author. Laboratory of Translational Psychiatry, Department of Psychiatry and Psychotherapy, Johannes Gutenberg University Medical Center Mainz, Hanns-Dieter-Hüsch-Weg 19, 55128, Mainz, Germany.

** Corresponding author. Laboratory of Translational Psychiatry, Department of Psychiatry and Psychotherapy, Johannes Gutenberg University Medical Center Mainz, Hanns-Dieter-Hüsch-Weg 19, 55128, Mainz, Germany.

E-mail addresses: daherzog@uni-mainz.de (D.P. Herzog), marianne.mueller@uni-mainz.de (M.B. Müller).

¹ Shared first authorship.

monitoring or drug choice in the clinical setting is a major drawback in depression treatment (Labermaier et al., 2013).

In search for putative targets mediating a more rapid antidepressant response, *N*-methyl-D-aspartate (NMDA) receptor antagonists, with ketamine as a prototypical agent, have gained increasing interest during the last years (Lener et al., 2017). Sub-anesthetic doses of the narcotic agent ketamine have been shown to produce both rapid (within hours) and sustained (up to 1 week) antidepressant effects in patients (Berman et al., 2000) and rodents (Browne and Lucki, 2013). In addition, there is convincing evidence from clinical trials that ketamine is also effective in patients with treatment-resistant depression (Schwartz et al., 2016). Besides its activity at the NMDA receptor, several putative molecular mechanisms through which the antidepressant-like effects of ketamine are mediated have been discovered, including the involvement of mechanistic target of rapamycin complex 1 (mTORC1) signaling and acute modulation of brain-derived neurotrophic factor (BDNF) release (Cavalleri et al., 2018).

Despite its proven antidepressant efficacy even in difficult-to-treat patients, a broad range of side effects, including strong sedation, dissociation, nausea, and the risk of addiction have prevented ketamine to be widely used so far (Short et al., 2018). Recent preclinical studies indicate that a ketamine metabolite, (2*R*,6*R*)-hydroxynorketamine (HNK), retains the rapid and sustained antidepressant-like effects in rodents, but lacks its dissociative-like properties and abuse potential (Chou et al., 2018; Pham et al., 2018; Zanos et al., 2016). Therefore, HNK is a potential prototypical candidate to be further tested and developed as a rapid-acting antidepressant agent. However, for HNK, which does not block NMDA receptors like ketamine (Lumsden et al., 2019), the molecular signaling mechanisms still remain largely unknown (Zanos et al., 2018). In addition, the antidepressant-like effects of HNK could not always be reproduced by research groups around the world. We summarized the evidence in a recent review (Herzog et al., 2019). To date, systematic studies aiming at the hypothesis-free identification of proteins and signaling pathways involved in HNK's rapid onset of action are yet to be reported.

Despite considerable efforts, biomarker candidates to support clinical diagnosis or treatment response that could finally support decision-making within MDD diagnosis and therapy guidelines are still lacking (NICE, 2018). Access to the organ of interest as source for biomaterial, i. e. the brain, is restricted, if not impossible. Data on peripheral blood-based biomarkers and molecular candidates have been relatively inconclusive so far, and peripheral changes are remarkably different from the molecular changes that are observed within the central nervous system (e.g. Carrillo-Roa et al., 2017). Cerebrospinal fluid (CSF) is an accessible biological fluid in both humans and rodents that is circulating in close vicinity to the brain. In the past decade, technological advancement and the increasing quality of unbiased "omics" approaches have facilitated the use of CSF for biomarker research and investigations into disease-related pathophysiological processes. However, in contrast to other mental diseases such as neurodegenerative disorders where CSF is traditionally an established source for biomarker research, only very few investigations have used CSF to monitor the changes in the context of antidepressant treatment.

In 2014, Onaivi et al. described an animal experimental approach using intraventricular cannulation to enable serial CSF withdrawal in conscious mice (Onaivi et al., 2014). The suitability of this approach was validated by revealing specific proteomic signatures in murine CSF samples following acute stress and acute cocaine administration (Onaivi et al., 2014). In the current study, we adopted this method to focus on temporal changes of the CSF proteome induced by systemic administration of an antidepressant-like dosage of HNK. As animal model system, we chose male DBA/2J mice. This inbred mouse strain is characterized by high innate anxiety, which turns them in an ideal translational model for depression with anxious distress, a diagnostic specifier of DSM-5. The mouse model can be successfully "treated" by commonly used antidepressants (Carrillo-Roa et al., 2017; Sillaber et al.,

2008; Sugimoto et al., 2011). Moreover, DBA/2J mice display a reduced inhibitory HPA axis feedback (Thoeringer et al., 2007) closely mimicking this impairment in patients suffering from MDD. Choosing an antidepressant-responsive strain enables experiments to be performed under baseline conditions i.e. without the need to apply additional and potentially confounding stressors to shift the behavioral phenotype of the animals to a depressive-like state to model disease-like conditions (Carrillo-Roa et al., 2017). Here, we performed serial CSF sample collection from conscious and freely moving mice in a longitudinal study design to identify the proteome changes closely associated with changes in brain states following administration of HNK over time. Changes in the CSF proteome and differential expression of proteins associated with the acute (4 h after injection) and sustained (1 week after injection) antidepressant-like effects of a single injection of HNK or saline were further investigated employing a hypothesis-free, unbiased mass spectrometry-based proteomics approach.

2. Materials and methods

2.1. Animals

Male, adult (8 weeks) DBA/2J mice were purchased from Charles River, France. After arrival at our animal facility, we single-housed all the mice (temperature = $22 \pm 2^\circ\text{C}$, relative humidity = $50 \pm 5\%$) and allowed them to habituate to the new environment for at least one week prior to any experiments. We applied a standard 12h dark/light cycle (8am – 8pm light, 8pm – 8am dark). Mice had *ad libitum* access to water and food. All experiments were conducted in accordance with European animal welfare laws and approved by the local animal welfare authority (Landesuntersuchungsamt Rheinland-Pfalz, Koblenz, Germany).

2.2. Drug administration

Murine body weight (BW) was measured 24 h before drug administration. Mice received ketamine hydrochloride (Inresa Arzneimittel GmbH, Germany; 30 mg/kg BW, based on (Browne and Lucki, 2013)), (2*R*,6*R*)-hydroxynorketaminehydrochloride (Tocris, Germany; 10 mg/kg BW, based on (Zanos et al., 2016)), or saline control (0.9% NaCl, Braun, Germany) intraperitoneally.

2.3. Behavioral assessment

2.3.1. Forced swim test (FST)

Mice ($n = 30$) were handled for 2 min daily for three consecutive days. We then injected them once with either ketamine or HNK or saline. We performed the FST to assess depressive-like behavior 4 h and 1 week after injection. Mice were introduced into a 2-L glass beaker (diameter 13 cm, height 24 cm) filled with tap water ($21 \pm 1^\circ\text{C}$) to a height of 15 cm. We videotaped the mice for 5 min and floating, swimming, and struggling behavior was scored by an experienced, observer blinded towards the treatment.

2.3.2. Open field test (OF)

In a new and independent experiment, mice ($n = 30$) were handled for 2 min daily for three consecutive days. We then injected them once with either ketamine or HNK or saline and immediately placed them into the OF arena ($45 \times 45 \times 41$ cm). We performed the OF to assess locomotor activity. Mice could move freely and without disturbance for 30 min, during which they were videotaped from above. Distanced moved was automatically scored with the tracking software Observer XT12 (Noldus, The Netherlands).

2.4. Blood plasma extraction

We withdrew blood *via* tail nicks into EDTA-coated tubes, as previously described (van der Kooij et al., 2018). We centrifuged all tubes for

10 min at 10 000 g at 4 °C and stored the plasma at –80 °C until further use.

2.5. Corticosterone (CORT) plasma concentration

We measured CORT plasma levels using the Corticosterone ELISA Kit (cat.no. ADI-900-0979; Enzo Life Sciences, USA) according to the manufacturer's protocol in duplicates.

2.6. Statistics of behavioral experiments and neuroendocrine measurements

Data was plotted and descriptive statistics were applied to check for normal distribution of the data (D'Agostino & Pearson omnibus normality test). We analyzed data with a 1- or 2-way ANOVA followed by Bonferroni correction. Alpha was set at 5%, with p values < 0.05 considered statistically significant. Data was analyzed using Prism 5 software (GraphPad, USA). Sample sizes are indicated in the figure legends. The values are displayed as mean ± SEM.

2.7. CSF cannula surgery

Ketamine and HNK were equally effective with respect to their antidepressant-like efficacy. Due to the improved side-effect profile of HNK and the gap of knowledge about the neurobiological mechanisms mediating its antidepressant-like activity, we exclusively focused on HNK with respect to the proteome profiling of the CSF.

CSF cannula implantation was conducted in a modified way based on the method by Onaivi and colleagues (Onaivi et al., 2014). In brief, mice were anesthetized with Isoflurane (Forene®, AbbVie Deutschland GmbH, Germany) and received the analgesic drug Metacam (Boehringer Ingelheim Vetmedica GmbH, Germany) subcutaneously (0.5 mg/kg BW). The skin was opened and two small holes were drilled into the skull, followed by applying two screws. A third hole was drilled and the intraventricular cannula (internal cannula; Plastics One, USA) was implanted at bregma coordinates 0.0 AP/0.8 ML/–0.9 VD. Paladur dental cement (Kulzer, Germany) was used to secure the internal cannula to the screws and the skull. The skin lesion was closed and a dummy cannula (Plastics One, USA) closed the internal cannula. Subsequently, the mice received Metacam in the drinking water for one week. After recovery from surgery, mice received new water bottles without the analgesic drug.

2.8. CSF withdrawal and protocol of the main experiment

Mice (n = 60) were handled carefully for 2 min per day for 1 week. CSF was withdrawn from all mice and the first sample was discarded to exclude contamination with blood. After three days, mice were randomized into an HNK or saline arm (Data file S1). They received an intraperitoneal injection of either HNK or saline and CSF samples were taken 4 h and 1 week after injection.

CSF withdrawals were conducted as follows: Dummy cannula was removed and tubing (5–10 cm in length; Plastics One, USA) with external cannula (additional –1.0 VD (final depth –1.9 VD); Plastics One, USA) was connected to the internal of the cannula at one end and to a 10 µl Model 701 N Hamilton syringe (cat.no. 80365; Hamilton, USA) at the other end. By gently pulling the plunger in steps of 1 µl for each 1 min, CSF was withdrawn. After the plunger reached 10 µl, CSF was collected and directly put on dry ice and later stored at –80 °C until further analyses. CSF-containing tubes were visually inspected for any blood contamination and excluded if necessary.

2.9. Proteomics sample preparation

The average volume obtained from all CSF samples was generally very low (5.7 ± 1.7 µl). Hence, the samples were pooled equally to a

total of 40 µl per biological replicate for the proteomics analysis, as described in data file S1. The designated samples were then subjected to one-dimensional gel electrophoresis (1DE) employing precast NuPAGE 4–12% Bis-Tris 10-well mini protein gels (Invitrogen, Germany) with 2-[N-morpholino]ethanesulfonic acid (MOPS) running buffer under reducing conditions at a constant voltage of 150V in 4 °C. Pre-stained protein standard, SeeBlue Plus 2 (Invitrogen, Germany), was used as a molecular mass marker and the gels were stained with Colloidal Blue Staining Kit (Invitrogen, Germany), as per manufacturer's instructions. The bands in each stained gel were sliced into 14 gel slices per lane with the aim to reduce the complexity and masking effect of the abundant proteins during the MS analysis (Fig. S2). Protein bands were excised (14 bands per replicate) Subsequently, all the excised protein bands were destained, reduced and alkylated prior to in-gel trypsin digestion employing sequence grade-modified trypsin (Promega, USA), as described in detail elsewhere (Manicam et al., 2018; Perumal et al., 2019, 2020). Peptides extracted from trypsin digestion were purified with ZipTip C18 pipette tips (Millipore, Billerica, MA, USA) according to the manufacturer's instructions. The resulting combined peptide eluate was concentrated to dryness in a centrifugal vacuum evaporator (SpeedVac) and dissolved in 10 µl of 0.1% trifluoroacetic acid (TFA) for liquid chromatography-electrospray ionization-tandem mass spectrometry (LC-ESI-MS/MS) analysis.

2.10. Discovery proteomics strategy

Peptide fractionation was conducted in the LC system, which consisted of a Rheos Allegro pump (Thermo Scientific, USA) and an HTS PAL autosampler (CTC Analytics AG, Switzerland) equipped with a BioBasic C18, 30 × 0.5 mm precolumn (Thermo Scientific, USA) connected to a BioBasic C18, 150 × 0.5 mm analytical column (Thermo Scientific, USA). Solvent A consisted of LC-MS grade water with 0.1% (v/v) formic acid and solvent B was LC-MS grade acetonitrile with 0.1% (v/v) formic acid. The gradient was run for 60 min per sample as follows: 0–35 min: 15–40% B, 35–40 min: 40–60% B, 40–45 min: 60–90% B, 45–50 min: 90% B, 50–53 min: 90–10% B: 53–60 min: 10% B.

The continuum MS data were obtained on an ESI-LTQ Orbitrap XL-MS system (Thermo Scientific, Bremen, Germany). The general parameters of the instrument were set as follows: positive ion electrospray ionization mode, a spray voltage of 2.15 KV and a heated capillary temperature of 220 °C. Data was acquired in an automatic dependent mode whereby, there was automatic acquisition switching between Orbitrap-MS and LTQ MS/MS. The Orbitrap resolution was 30000 at m/z 400 with survey full scan MS spectra ranging from an m/z of 300–1600. Target automatic gain control (AGC) was set at 1.0×10^6 ion. Internal recalibration employed polydimethylcyclosiloxane (PCM) at m/z 445.120025 ions in real time and the lock mass option was enabled in MS mode (Olsen et al., 2005). Tandem data was obtained by selecting top five most intense precursor ions and subjected them for further fragmentation by collision-induced dissociation (CID). The normalized collision energy (NCE) was set to 35% with activation time of 30 ms with repeat count of three and dynamic exclusion duration of 600 s. The resulting fragmented ions were recorded in the LTQ. The acquired continuum MS spectra were analyzed by MaxQuant computational proteomics platform version 1.6.3.3 and its built-in Andromeda search engine for peptide and protein identification (Cox et al., 2011, 2014; Cox and Mann, 2008; Luber et al., 2010; Tyanova et al., 2016). The tandem MS spectra were searched against UniProt *Homo sapiens* (Date, Oct 17, 2018; 20 410 proteins listed) and *Mus musculus* (Date, Oct 17, 2018; 17 001 proteins listed) databases, using standard settings with peptide mass tolerance of ±30 ppm, fragment mass tolerance of ±0.5 Da, with ≥6 amino acid residues and only “unique plus razor peptides” that belong to a protein were chosen (Cox and Mann, 2008). Both the *Mus musculus* and *Homo sapiens* databases were utilized with the aim to maximize the protein identification due to limited availability of annotated mouse proteins in a specific database (Perumal et al., 2020). A

target-decoy-based false discovery rate (FDR) for peptide and protein identification was set to 0.01. Carbamidomethylation of cysteine was set as a fixed modification, while protein N-terminal acetylation and oxidation of methionine were defined as variable modifications, enzyme: trypsin and maximum number of missed cleavages: 2. The generated MaxQuant output data table “proteingroups.txt” was filtered for reverse hits prior to statistical analysis and, subsequent functional annotation and pathway analyses. The summary of MaxQuant parameters employed in the current analyses is tabulated in data file S2.

2.11. Bioinformatics and functional annotation and pathways analyses

The output of the generated “proteingroups.txt” data from the MaxQuant analysis was utilized for subsequent statistical analysis with Perseus software (version 1.6.1.3). First, all raw intensities were \log_2 -transformed and the data were filtered with minimum of three valid values in at least one group and the missing values were imputed by replacing from normal distribution (width: 0.3; down shift: 1.8)), enabling statistical analysis (Tyanova et al., 2016). For statistical evaluation, a two-sided Student’s t-test was used for the group comparison with p-values < 0.05 to identify the significantly differentially abundant proteins. Unsupervised hierarchical clustering analysis of the differentially expressed proteins was conducted with \log_2 fold ratio of the protein intensities according to Euclidean distance (linkage = average; preprocess with k-means) and elucidated in a heat map. The overlaps of the statistically differentially expressed proteins between the databases utilized were manually curated based on the highest significance values. The list of the identified proteins was tabulated in Excel and their gene names were used for subsequent functional annotation and pathways analyses employing Ingenuity Pathway Analysis (v01-04, IPA; Ingenuity QIAGEN Redwood City, CA) (<https://www.qiagenbioinformatics.com/products/ingenuity-pathway-analysis>) (Kramer et al., 2014). IPA analyses unraveled the protein-protein interaction (PPI) networks, identified the significantly affected canonical pathways, top disease and functions, and predicted upstream regulators associated with the proteins identified to be differentially expressed. Top canonical pathways of the differentially expressed proteins were presented with p-value calculated using Benjamini-Hochberg (B-H) multiple testing correction ($-\log B-H > 1.3$) and a cut-off of ≥ 3 affected proteins per pathway. In PPI networks, proteins molecules are represented by their corresponding gene names and, only PPIs that were experimentally observed and had direct and indirect interactions were used.

2.12. In vitro GR activity and gene reporter assays

HT-22 mouse hippocampal neuronal cell line was used as an *in vitro* model to analyze the molecular effects of HNK on GR transcriptional activity and GR sensitivity to glucocorticoids. Experiments were conducted as described before (Schulke et al., 2010; Touma et al., 2011). Briefly, cells were cultivated, transfected with MMTV-Luc and Gaussia-Luc expression constructs using Lipofectamine 2000 (ThermoFisher) and treated with HNK in concentrations of 0.1 μ M, 1.0 μ M, 10.0 μ M, and 30.0 μ M ($n = 3$ per group). Two conditions using culture medium (DMEM, Gibco) supplemented with either standard fetal bovine serum as or with charcoal stripped serum as steroid-free condition were examined to observe HNK effects on the GR-driven transcriptional activity. For evaluating the GR response to hormonal activation, GR-agonist dexamethasone (0.1 nM, 0.3 nM, 1 nM, 3 nM, 10 nM, 30 nM, 100 nM) was added and cells were treated with either HNK (5 μ M) or vehicle. Data were analyzed using 2-way ANOVA followed by Bonferroni correction. Alpha was set at 5%, with $p < 0.05$ considered statistically significant. Data was analyzed using Prism 5 software (GraphPad, USA).

3. Results

3.1. Behavioral profiling of ketamine and HNK in DBA/2J mice

With this behavioral experiment, we wanted to first validate that DBA/2J inbred mice are a suitable strain and model organism to investigate the antidepressant-like effects of ketamine and HNK. DBA/2J mice displayed a depression-like phenotype under control conditions with high immobility scores in the FST (Fig. 1A and B at 4h and 1w, respectively; saline-treated animals). At both *acute* and *sustained* time points, ketamine and HNK induced significant antidepressant-like effects by reducing immobility time (Fig. 1A and B). We detected no statistically significant differences between the effects of HNK and ketamine at both time points (Fig. 1A and B).

Locomotor activity is known to be impaired by ketamine treatment and constitutes an important side-effect of ketamine (Short et al., 2018). Indeed, an acute, ketamine-induced reduction in general locomotor activity could be visualized by an altered tracking profile in the OF test during 30 min of post-injection recording (Fig. 1C). Furthermore, ketamine reduced the total distance travelled, compared to HNK and saline injection (Fig. 1D).

3.2. Acute and sustained effects of HNK on CSF proteome

CSF is in close vicinity to the brain, and there is a continuous exchange and molecular crosstalk between brain tissue and CSF. Because of the clear behavioral effects of HNK and the fact that so far, data about its mechanism of action remain fragmentary, we decided to exclusively focus on HNK and analyze the CSF samples obtained from conscious DBA/2J mice treated with HNK or saline. As part of the method validation, we investigated whether the CSF withdrawal procedure was stressful for the animal by measurement of plasma CORT concentrations in an independent experiment. The mean peak level of CORT from mice which underwent the CSF withdrawal procedure was 84.84 ng/ml (Fig. S1), not exceeding average plasma CORT concentrations reached following exposure to a novel environment, such as a commonly used OF test (Gentsch et al., 1981).

In the main experiment, CSF samples were pooled (Data file S1), processed, and subjected to first dimensional gel electrophoresis (1DE; Fig. S2). In total, 387 proteins were identified from both *Mus musculus* (309 proteins) and *Homo sapiens* (229 proteins) databases by label-free quantification at a false discovery rate (FDR) of 1% (Fig. 2A; full data in data files S3–S5). As many as 151 proteins were found to be overlapping in both databases, as shown in the Venn diagram (Fig. 2A). The use of both mouse and human UniProt databases maximized protein identification due to limited annotations in the mouse database (17 001 proteins) compared to the human database (20 410 proteins).

Among these murine CSF proteins, 25 and 65 proteins were found to be differentially expressed at 4 h (Fig. 2B) and 1 week (Fig. 2C) after HNK treatment compared to saline (for comprehensive list see data file S6 and Fig. S3). Nine proteins were upregulated following 4 h HNK administration namely cytoskeletal structural protein dynein light chain 2, cytoplasmic (Dylnl2), proteasome subunit beta type 2 (Psm2), apolipoprotein (ApoE), and spine growth modulator protein transforming protein RhoA (RhoA). Sixteen proteins were downregulated following 4 h HNK versus saline injection (Fig. 2C), mainly cytoskeletal keratins consisting of keratin type II cytoskeletal 1, 2 peridermal, 2 oral, 9, 10 (KRT1, KRT2, KRT76, KRT9, KRT10), myelin proteins composed of myelin basic protein (Mbp) and myelin proteolipid protein (Plp1), signaling protein 14-3-3 protein sigma (Sfn), and myelinotrophic and neurotrophic factor prosaposin (Psap). One week following HNK injection, we found 41 proteins to be upregulated (Fig. 2C). Examples of these proteins were Mbp, Plp1, glial fibrillary acidic protein (Gfap), amino acid transporters ADP/ATP translocase 2 (SLC25A5) and 1 (Slc25a4), cytoskeletal proteins actin-related protein 2/3 complex subunit 4 (Arpc4), vimentin (Vim), tubulin beta-5 chain (Tubb5), plasma

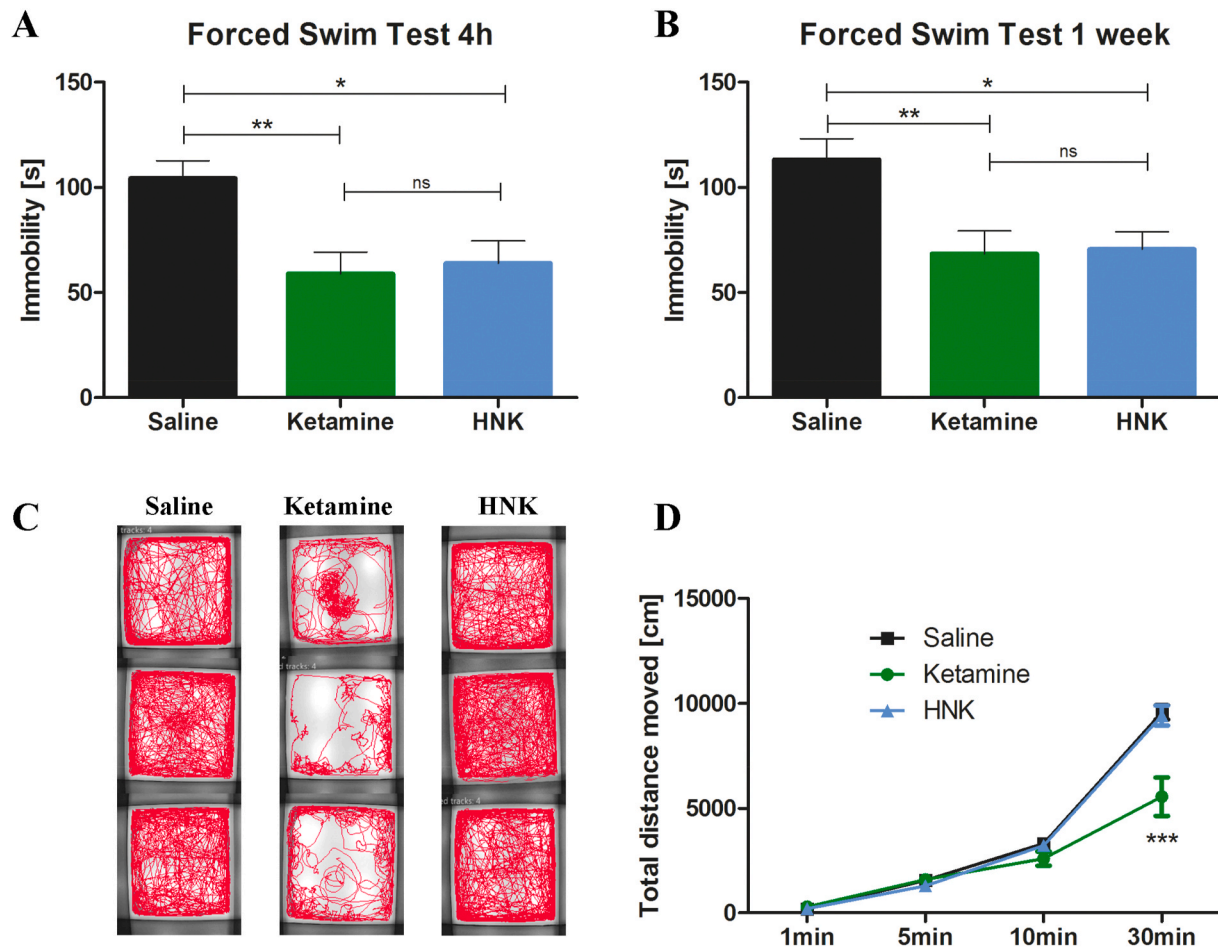


Fig. 1. Antidepressant-like effects and side-effects of ketamine and HNK. (A) 4 h after injection, ketamine [$t = 3.32$, $p < 0.01$] and HNK [$t = 2.96$, $p < 0.05$] reduced immobility time in the FST [$F = 7.44$, $p = 0.0019$, $n = 10$ per group]. (B) 1 week after injection, ketamine [$t = 3.24$, $p < 0.01$] and HNK [$t = 3.08$, $p < 0.05$] reduced immobility time in the FST [$F = 6.67$, $p = 0.0044$, $n = 10$ per group]. (C + D) Ketamine affected locomotor activity [$n = 10$ per group]. (C) Ketamine-treated mice show an altered tracking profile [3 examples per group]. (D) Ketamine decreased locomotor activity [Interaction: $F = 13.32$, $p < 0.001$; time: $F = 388.8$, $p < 0.001$; treatment: $F = 7.65$, $p < 0.01$] compared to HNK [$t = 7.79$, $p < 0.001$] and saline [$t = 8.10$, $p < 0.001$] [$n = 10$ per group]. ns not statistically significant, HNK (2R,6R)-hydroxynorketamine, * $p < 0.05$, ** $p < 0.01$, *** $p < 0.001$, bars are depicted as mean \pm SEM, one-way ANOVA with Bonferroni posttest in A + B, two-way repeated-measures ANOVA with Bonferroni posttest in D.

kallikrein (Klkb1), moesin (Msn), and transcription factor putative elongation factor 1-alpha-like 3 (EEF1A1P5). A total of 24 proteins were downregulated comprising mainly cytoskeletal keratins (KRT1, 9, 6A, 10), mitochondrial proteins electron transfer flavoprotein subunit alpha (ETFA), malate dehydrogenase (Mdh2), stress-70 protein (HSPA9), 4-aminobutyrate aminotransferase (Abat), aconitate hydratase (Aco2), pyruvate dehydrogenase E1 component subunit beta (PDHB), Na/K-transporting ATPase subunit alpha-1 (ATP1A1), cholinergic neuron ATP-binding protein in neurons phosphatidylethanolamine-binding protein 1 (Pebp1), and chaperone heat shock protein a5 (HSPA5). Further clustering of these differentially expressed CSF proteins depicted as heat maps with unsupervised hierarchical clustering demonstrated the segregation of identified proteins into two major clusters according to the respective time points (Fig. 2D). Three distinct protein expression profiles were observed. First, the expression of a cluster of proteins remained the same at both 4h and 1w composed of down-regulation of KRT1, KRT9, and KRT10, and the up-regulation of Rbp4. The second cluster consisted of proteins that were upregulated following 1w of HNK administration comprising Mbp and PLP1. The third cluster was characterized by expression of proteins that were only regulated exclusively at either time point. Conducting a protein-protein interaction network (PPI) analysis, we could show the localization in particular cellular compartments and molecular types (Fig. S3). Interestingly, the protein

group observed to have the highest interaction partners consisted of keratins (Fig. S3).

In an attempt to further explore the functional relevance of the proteins identified to be differentially expressed, canonical pathway enrichment was determined employing the IPA tool using a cut-off of $p < 0.05$. The 21 proteins following 4 h HNK injection were significantly associated with the glucocorticoid receptor (GR) signaling ($p = 1.52E-03$; Fig. 3A). On the other hand, 9 top canonical pathways were found to be differentially regulated by the 57 differentially expressed proteins following 1 week HNK treatment (Fig. 3A). Among these, the acute phase response signaling ($p = 5.30E-11$; Fig. 3B) was the most significantly implicated pathway, followed by GR signaling ($p = 2.35E-03$; Fig. 3C), unfolded protein response ($p = 3.07E-04$; Fig. 3D), glycolysis I ($p = 1.21E-02$; Figs. 3E), and 14-3-3 mediated signaling ($p = 3.68E-03$; Fig. 3F). Noteworthy, the GR signaling-associated proteins at both time points comprised mainly a cluster of keratins and heat shock proteins. Among the keratins, KRT1, KRT9, and KRT 10 were consistently downregulated at both time points, whereas KRT76 and KRT2 were exclusively downregulated at 4 h and KRT6A at 1 week after HNK treatment (Fig. 3B; Data file S7).

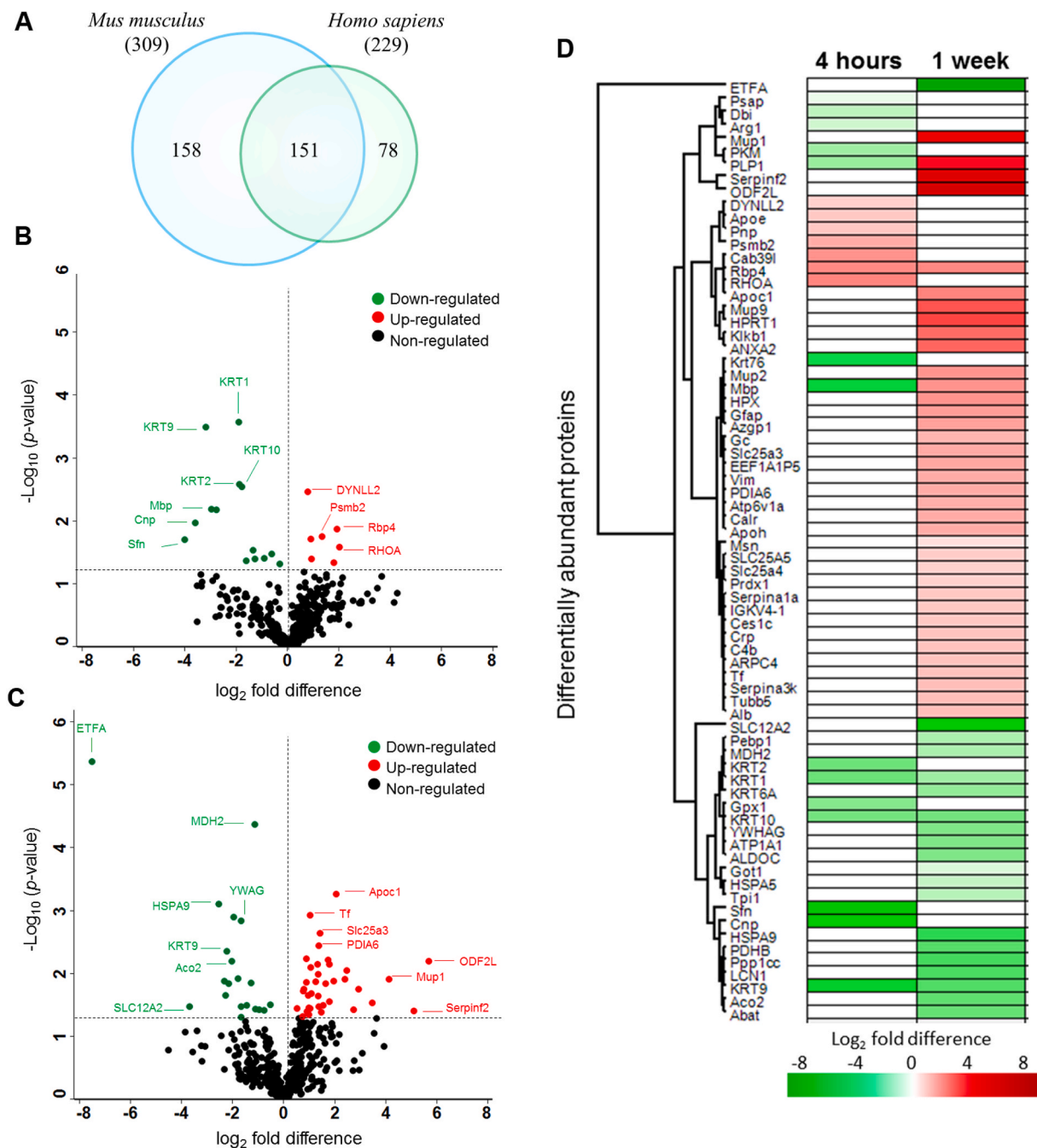


Fig. 2. Acute and sustained effects of HNK on CSF proteome. (A) Venn diagram depicts the total number of proteins identified in both mouse and human databases in the CSF samples. Volcano plot illustrates significantly differentially abundant CSF proteins after (B) 4 h and (C) 1 week HNK administration compared to saline. The negative log₁₀ (p-value) is plotted against the log₂ (fold change: HNK/saline). The non-axial horizontal line denotes p = 0.05, which is our significance threshold (prior to logarithmic transformation). Significantly upregulated proteins are plotted in red, while proteins that were downregulated by HNK are represented in green and non-regulated proteins are in black (D) The hierarchical clustering of the differentially expressed CSF proteins at 4 h and 1 week after HNK treatment displayed in a heat map. The upregulated proteins are shown in red and the downregulated proteins are in green, with log₂ fold difference of intensity displayed in color (green/red). n = 60 mice, after pooling n = 3 per group (for details of pooling see Data file S1). (For interpretation of the references to color in this figure legend, the reader is referred to the Web version of this article.)

3.3. HNK represses GR-mediated transcription and reduces hormonal sensitivity of GR in vitro

We were interested how HNK affected GR translational activity and GR response to glucocorticoids in neuronal cells. We performed an *in vitro* gene reporter assay assessing GRE-driven transcriptional activity by transient transfection of MMTV-Luciferase construct into HT-22 mouse hippocampal neuronal cells and found that HNK represses GR-mediated

transcription in a glucocorticoid (DEX) dependent manner (Fig. S4). We detected no direct effect of HNK on GR-activity, when steroids were withdrawn from culture medium (Fig. S4). Moreover, we found a reduced hormonal sensitivity of GR when cells were co-treated with HNK compared to control condition (Fig. 3G).

A further analysis of the biological functions associated with the differentially expressed CSF proteins at both time points was conducted (Fig. 4A). At 4h after HNK treatment, organization of filaments (p =

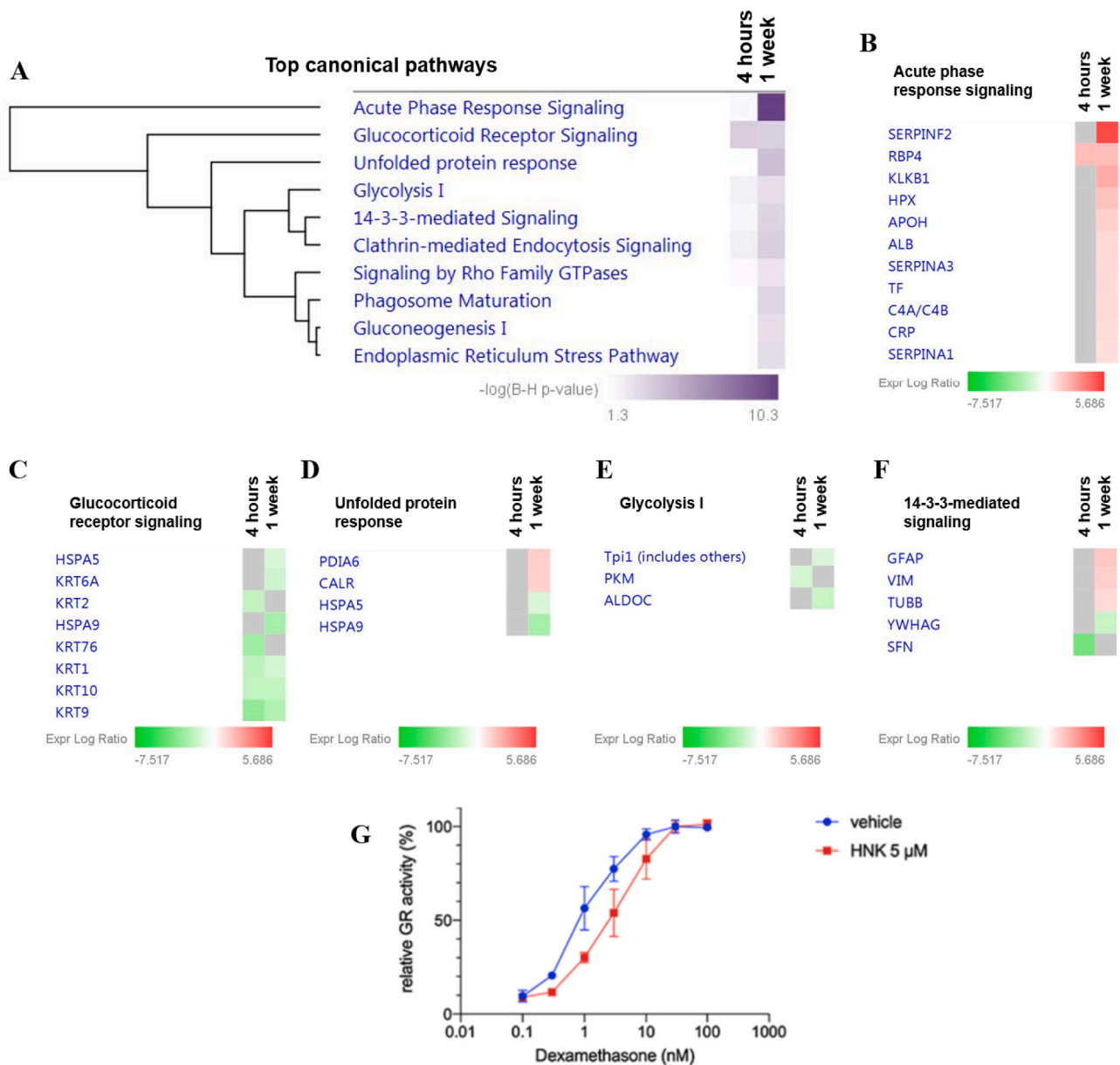


Fig. 3. Top enriched canonical pathways of the differentially expressed proteins significantly affected by HNK treatment. (A) The significantly enriched canonical pathways determined by IPA's default threshold [$-\log(B-H \text{ p-value}) > 1.3$] between the differentially expressed proteins identified in our datasets and the molecules in the respective pathways at 4h and 1w time-points following HNK treatment. Proteins associated with respective canonical pathways and their expression profiles at 4 h and 1 w are as follows; B) acute phase response signaling C) glucocorticoid receptor signaling, D) unfolded protein response, E) glycolysis I and F) 14-3-3-mediated signaling. The intensity of the color (green/red) indicates the degree of \log_2 fold ratio of each protein. G) Relative GR activity was reduced through HNK (5 μ M) treatment compared to vehicle control administration ($p < 0.05$ for 1.0 nM dexamethasone treatment). Relative receptor activity represents firefly luciferase activity (MMTV-promoter) normalized to Gaussia luciferase activity and is represented to the activity at saturating 30 nM dexamethasone. 2-way ANOVA followed by Bonferroni correction was applied. $n = 3$ per group. (For interpretation of the references to color in this figure legend, the reader is referred to the Web version of this article.)

1.04E-02; Fig. 4B), myelination ($p = 2.43E-03$; Fig. 4C) and regeneration of neurons ($p = 4.32E-03$; Fig. 4D) were found to be significantly affected. The subacute effect of HNK administration after 1w demonstrated that the proteins found to be differentially expressed were significantly associated with top four networks involved in organization of filaments ($p = 6.36E-05$; Fig. 4B), gluconeogenesis ($p = 7.17E-04$; Fig. 4E), proliferation of neuroglia ($p = 2.01E-03$; Fig. 4F) and regeneration of neurons ($p = 1.75E-02$; Fig. 4D).

Finally, we analyzed the predicted upstream regulators to identify the molecules, including transcription factors, which were significantly involved in the downstream regulation of the differentially expressed proteins in both groups (Fig. 5A and Fig. 6A). The major regulators at the

4h time point were tumor necrosis factor (TNF) ($p = 1.6E-04$; Fig. 5B), mTOR ($p = 1.2E-05$; Fig. 5C) and insulin like growth factor 1 (IGF1) ($p = 7.7E-05$; Fig. 5D). Interestingly, the mechanistic network analysis of the aforementioned upstream regulators were predicted to be inhibited (IGF1, $z\text{-score} = -2.18$; TNF, $z\text{-score} = -0.743$; mTOR, $z\text{-score} = -0.475$) at the 4h time point, (Fig. 6A). Elucidation of the interaction networks of the mechanistic inhibition demonstrated that these upstream regulators were regulated based on the decreased expression of seven proteins, namely, SFN, CNP, PLP1 and Mbp (Fig. 6B). Meanwhile, the major regulators at the 1w time point were TNF ($p = 3.9E-03$; Fig. 5B), mTOR ($p = 1.2E-03$; Fig. 5C), IGF1 ($p = 1.7E-04$; Fig. 5D), BDNF ($p = 1.2E-04$; Fig. 5E) and interleukin 6 (IL6) ($p = 1.2E-05$;

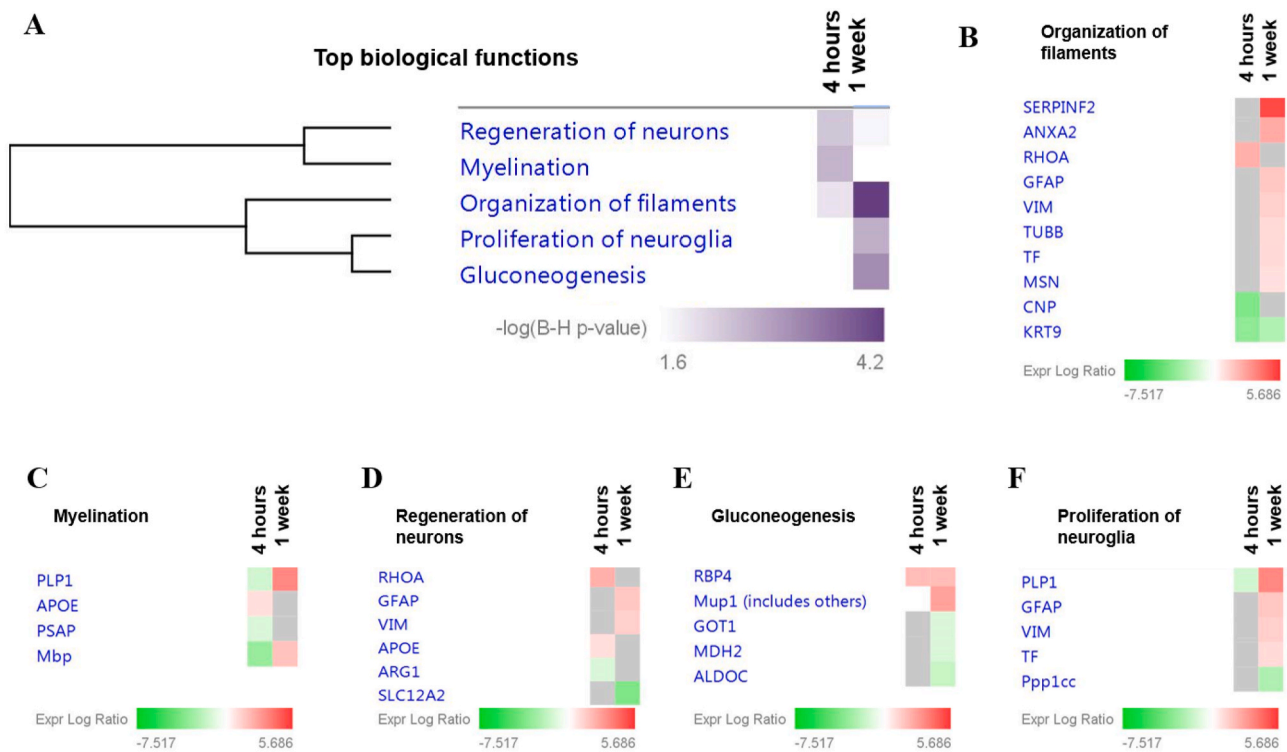


Fig. 4. Functional classification of the differentially expressed CSF proteins according to the enriched top diseases and biological functions. (A) Comparison analysis of the significantly affected diseases and biological functions between both time-points following HNK administration. The significance threshold [$-\log(B-H \text{ p-value}) > 1.6$] was determined by IPA analysis. Proteins associated with respective biological functions and their expression profiles at 4 h and 1 w are as follows; (B) Organization of filaments, (C) proliferation of neuroglia, (D) gluconeogenesis, (E) myelination and (F) regeneration of neurons. The intensity of the color (green/red) indicates the degree of \log_2 fold ratio of each protein. (For interpretation of the references to color in this figure legend, the reader is referred to the Web version of this article.)

(Fig. 5F). Intriguingly, the mechanistic network analysis of the upstream regulators at 1w was predicted to be activated (TNF, z -score = 0.742; mTOR, z -score = 0.243; IGF1, z -score = 1.28; BDNF, z -score = 0.128; IL6, z -score = 1.337) (Fig. 6A). Elucidation of the interaction networks of the mechanistic activation demonstrated that these upstream regulators were regulator based on the increased expression of 11 regulated proteins, namely, CRP, SERPINA3, HPRT1 and GFAP, as shown in figure Fig. 6C.

4. Discussion

The present study provides first evidence that the DBA/2J mouse strain is a suitable animal model to assess the antidepressant-like effects of rapid-acting antidepressants such as ketamine and HNK. In a next step, we successfully used this model to decode the molecular mechanisms underlying HNK's rapid acting properties: we characterized the signature and longitudinal changes in the CSF proteome of conscious mice following systemic injection of HNK, which is the most promising metabolite of ketamine. Mechanistically, we identified GR signaling as a putative novel candidate mechanism through which both acute and sustained antidepressant-like effects of HNK might be mediated, thus revealing an intriguing functional link between HNK's antidepressant mechanism of action and targeted regulation of the stress hormone system.

4.1. Acute and sustained antidepressant-like properties of HNK: importance of experimental model system

In 2016, Zanos et al. first described the antidepressant-like properties of HNK (Zanos et al., 2016), which was then further investigated and developed as a putative rapid-acting antidepressant compound with a

more favorable side-effect profile than ketamine (Chou et al., 2018; Pham et al., 2018). However, while antidepressant-like effects of ketamine in rodents are relatively robust, the behavioral effects of HNK are more inconsistent and seem to depend on different parameters within the experimental conditions and the mouse strain used (Fitzgerald et al., 2019). Most of the recent studies on ketamine and HNK applied experimental depression models, such as stress or chronic inflammation (Herzog et al., 2019). For example, Chou et al. used a learned helplessness paradigm to induce a depressive-like phenotype in rats and demonstrated that HNK decreased depression-like behavior independent of gender (Chou et al., 2018). Another study using a lipopolysaccharide model of depression was not able to detect any antidepressant-like effects of HNK that were comparable to those of ketamine in male C57/BL6J mice (Yamaguchi et al., 2018). One plausible explanation for those inconsistencies of behavioral effects of HNK in rodents might be the use of different strains and experimental disease models and approaches to mimic clinically relevant conditions.

Adding to this, we could show for the first time, that a single dosage of HNK is equally effective as ketamine in inducing both acute and sustained antidepressant-like effects in DBA/2J mice. Saline-injected animals (i.e. vehicle controls) showed a depression-like behavioral phenotype, which could be attenuated by administration of ketamine and HNK. However, we acknowledge that reference data for the use of HNK and ketamine in the DBA/2J strain is still lacking. We analyzed only a single dose per agent based on published evidence (Browne and Lucki, 2013; Zanos et al., 2016), derived from studies with other mouse strains. The clear antidepressant-like effect of both compounds is probably due to the innate high anxiety-like behavior of this inbred mouse strain, which has proven its particular value in psychopharmacological research into antidepressant mechanisms of action (Carrillo-Roa et al., 2017). Therefore, it is surprising to see that for the

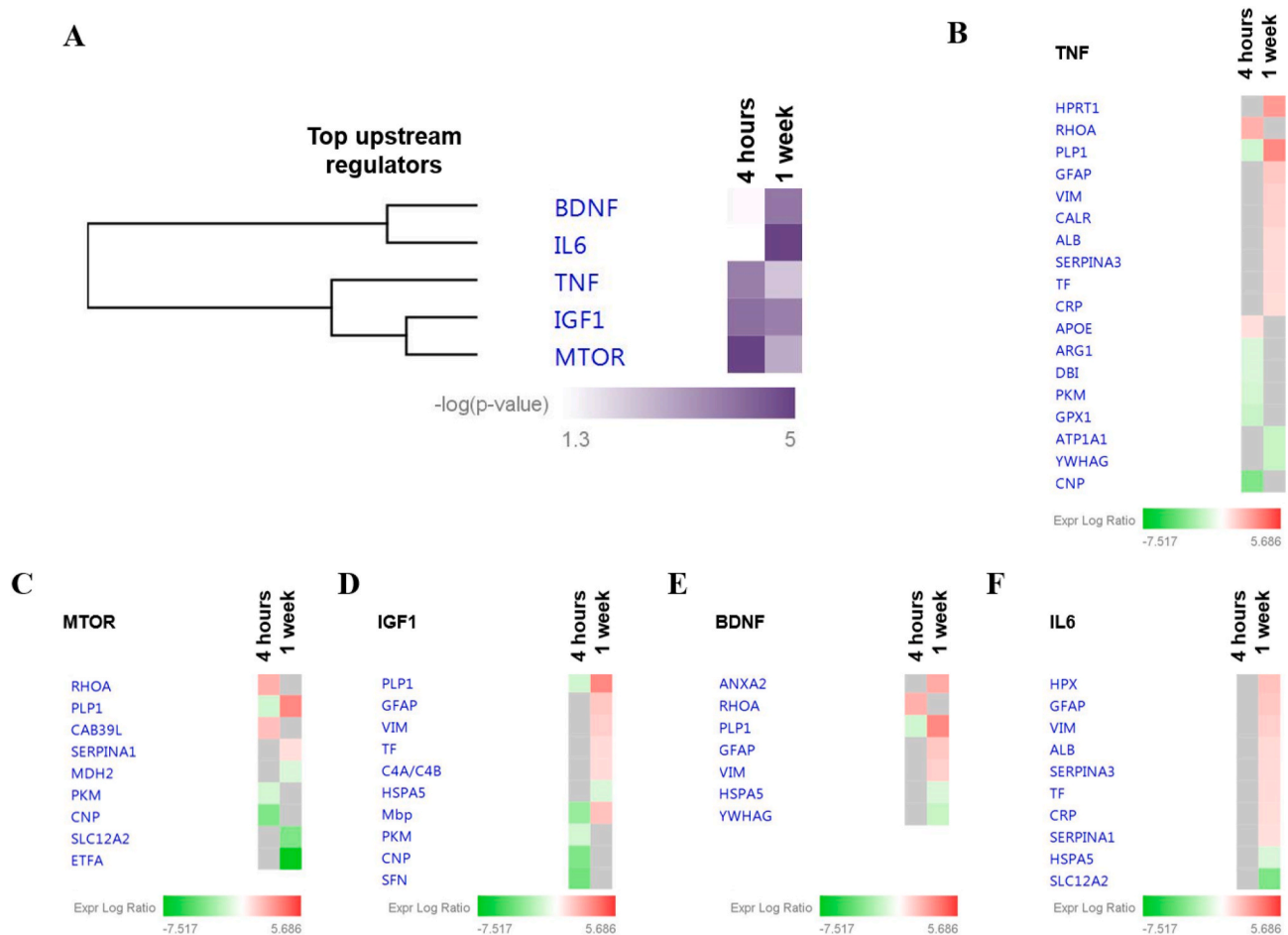


Fig. 5. Predicted top upstream regulators. (A) Hierarchical elucidation of the significantly affected potential upstream regulators observed to experimentally affect the differentially expressed CSF protein clusters at 4h and 1w. The significance threshold [$-\log(p\text{-value}) > 1.3$] was determined by IPA analysis. Proteins associated with the respective predicted upstream regulators and their expression profiles at 4 h and 1 w are as follows: (B) TNF, (C) mTOR, (D) IGF1, (E) BDNF and (F) IL6.

rapid-acting compound ketamine and its metabolite HNK, many studies published so far used the C57/BL6 strain, which, under baseline conditions, does not show a typical depression-like behavioral phenotype. Our data support that the DBA/2J strain is a suitable mouse model for studies into the neurobiology of rapid-acting antidepressant compounds. The majority of the published studies revealed antidepressant-like effects of ketamine 24 h after injection (Herzog et al., 2019). In addition, several studies have shown a sustained, lasting effect of ketamine up to two weeks (Brachman et al., 2016). This prompted us to analyze two different time points and we could indeed show that ketamine and HNK produced both acute (4 h) and sustained (1 week) antidepressant-like effect in male DBA/2J mice in the FST. Furthermore, ketamine administration significantly impaired locomotor activity, comparable to sedation and other related side-effects that can be prominently seen in patients (Short et al., 2018). HNK, in contrast, did not show an impact on locomotor activity in DBA/2J mice, supporting the fact that due to its favorable side-effects profile, HNK might be an ideal candidate to be further tested as rapid-acting antidepressant in clinical use. This prompted us to exclusively focus our in-depth proteomic analysis on HNK. However, an additional interpretation of the open field results might be that HNK at the dose used in this work might only acts as an antidepressant, whereas ketamine also might act as an anxiolytic agent reducing locomotor activity. Behavioral phenotypes observed in the open field test typically involve a mixture of emotional and anxiety-related components. In addition, we used a dose of 10 mg/kg BW for HNK and 30 mg/kg BW for ketamine. This might also be a reason

for the lack of impairment of locomotor activity of HNK.

4.2. Temporal CSF proteome profiles associated with antidepressant-like effects of HNK point to involvement of GR signaling as a putative mechanism of action

As CSF is an accessible biological fluid in both mice and humans that is circulating in close vicinity to the brain, this translational approach was intended to shed light on the molecular pathways underlying HNK's rapid and sustained antidepressant-like properties. Our results demonstrated that HNK induced time-dependent changes in the murine CSF proteome compared to vehicle-treated control mice.

Our data point, for the first time, to an important role of the GR signaling pathway in the rapid and sustained antidepressant-like properties of HNK. There is convincing evidence in the literature, both from human studies and experimental models, that depression is linked to a dysfunction of the hypothalamus-pituitary-adrenal (HPA) axis, finally resulting in increased levels of circulating glucocorticoids (Anacker et al., 2011). In particular, impaired GR signaling was discussed to be a key mechanism in the pathogenesis of depression (Holsboer, 2000), which is in line with the hypothesis that antidepressants reduce depressive symptoms by restoring HPA axis function (Anacker et al., 2011). For example, a recent study by Arango-Lievano et al. showed that the disruption of GR signaling in rats induced depression-like symptoms and that GR signaling was involved in modulating antidepressant-induced neuronal plasticity needed for reversal of

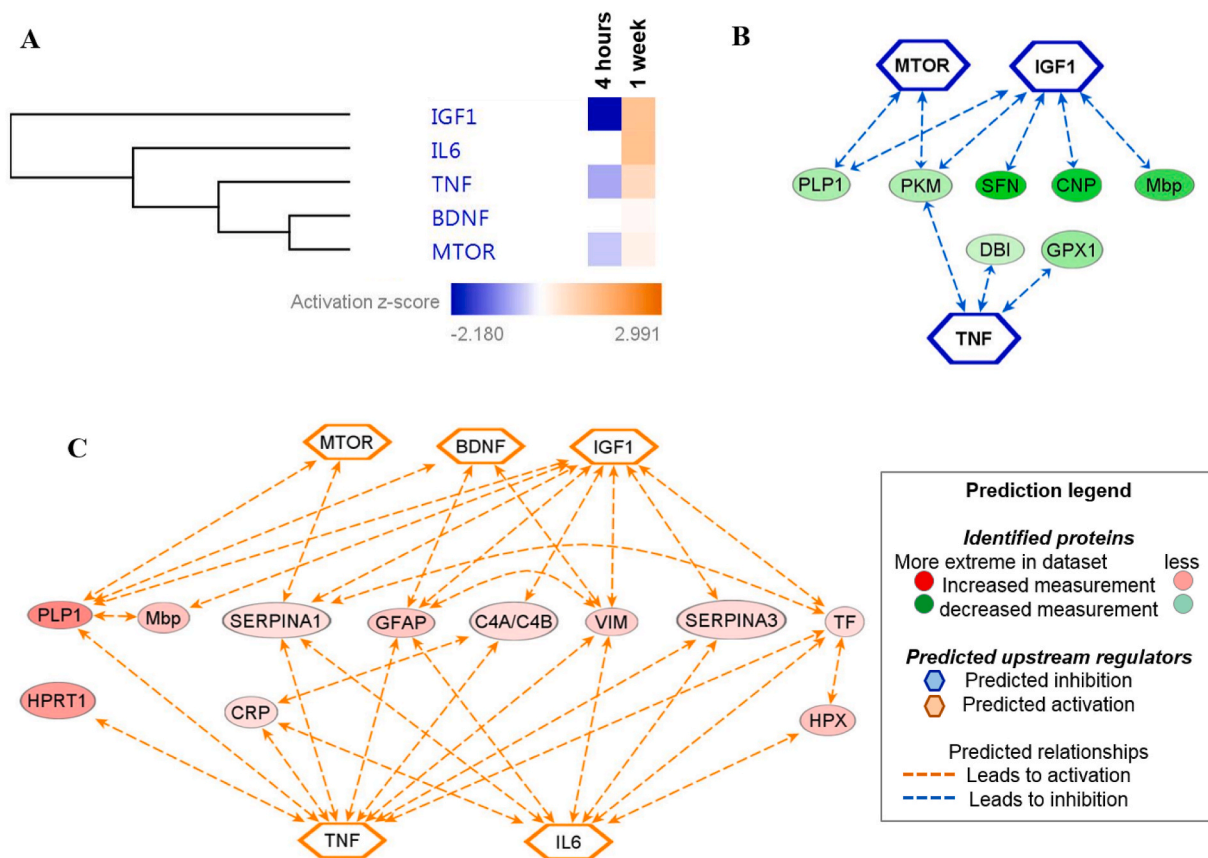


Fig. 6. Mechanistic network analysis of the predicted upstream regulators. (A) Hierarchical clustering of the significantly affected potential upstream regulators observed to experimentally affect the differentially expressed CSF protein clusters at 4h and 1w. The activation z-score of the regulators is depicted as orange (activated) and blue (inhibited), which was determined by IPA analysis. Elucidation of the interaction networks of the mechanistic activation/inhibition of the top significantly predicted upstream regulators and the associated regulated proteins at (B) 4h and (C) 1w.

depression-like symptoms (Arango-Lievano et al., 2015). While the close link between HPA axis activity and mechanism of action is well established for “classical” antidepressants such as tricyclic antidepressants or serotonin reuptake inhibitors, data on a putative involvement of the stress hormone system in mediating antidepressant-like effects of prototypical rapid acting compounds is sparse. For ketamine, it was described that in addition to its antidepressant-like properties, it was able to restore HPA axis function and to normalize peripheral CORT levels in a mouse chronic stress model (Wang et al., 2019). So far, data on a putative impact of HNK on modulating GR signaling was lacking. In addition to the proteomic profiling data pointing to an involvement of GR signaling, we here provide a first mechanistic insight into HNK’s effect on GR function: we could show, for the first time, that GR responsiveness *in vitro* was reduced following HNK treatment. Interestingly, a large majority of the proteins implicated in the GR signaling are composed of keratins and these structural proteins were found to be down-regulated following HNK treatment at both time points. Although keratins are traditionally associated with the skin (Toivola et al., 2015), their role in stress signaling has opened a new avenue in neurological disorders. This is supported by recent findings that provided compelling experimental evidence on the role of a specific keratin in CSF as a potential biomarker for Alzheimer’s disease (Richens et al., 2016). Furthermore, a study by Helenius et al. has lent support to the notion that the expression levels of different keratin subtypes are proportionate to stress in intestinal diseases (Helenius et al., 2016). Apart from keratins, heat shock proteins (HSPs) were also found to be similarly differentially expressed in stress conditions (Helenius et al., 2016). Correspondingly, our results have demonstrated that HSPA5 and HSPA9 were also downregulated in addition to the keratins at the 1w time point.

Therefore, based on these results, it is tempting to suggest that down-regulation of keratins and also HSPs in our mouse model reflect the HNK-mediated amelioration of stress and this effect lasted for as long as one week. Collectively, these results highlight the crucial effect of HNK in regulating the GR signaling in maintaining the homeostatic balance in the CSF proteome. Among the other differentially expressed candidate proteins, we found Dynll2 which plays a pivotal role in controlling cytoskeletal structures (Rapali et al., 2011) to be upregulated 4 h after HNK administration. The expression of several other cytoskeletal proteins like Arpc4, Vim, Tubb5, Klkb1, and Msn, which were associated with the organization of filaments, regeneration of neurons and proliferation of neuroglia, were also shown to be induced one week after HNK administration. These findings are in line with recent reports indicating the relevance of cytoskeletal dynamics in translating stressful environmental experiences into persistent changes of molecular and cellular function (Kretschmar et al., 2018; van der Kooij et al., 2016). The fact that we identified a considerable number of cytoskeletal proteins to be specifically regulated by HNK (i.e. putative targets of HNK) could point to their involvement in mediating rapid antidepressant-like effects, which is an intriguing hypothesis considering their crucial role in fine-tuning of synaptic plasticity and function (Cingolani and Goda, 2008). Moreover, we found proteins Mbp, Plp1, and Psap to be altered by HNK administration, with downregulation of Mbp and Plp1 at 4 h following HNK administration, and upregulation one week later. The latter are proteins playing important roles in myelination and myelin integrity (Campagnoni and Skoff, 2001). In fact, Weckmann and colleagues provided evidence that ketamine, the parent compound of HNK, increased Mbp protein levels in mice (Weckmann et al., 2019). Transcriptomics analysis of mouse choroid plexus have reported that the most

highly expressed genes in this tissue that secretes the CSF are involved mainly in energy metabolism (Sathyanesan et al., 2012). We have also identified several key proteins involved in glycolysis/gluconeogenesis, namely PKM, ALDOC, MDH2 to be associated with the treatment of HNK at 4h as well as at 1w.

In addition, the antidepressant-like effects of ketamine are known to take effect via enhancement of synaptogenesis: a single injection of ketamine triggered mammalian target of rapamycin (mTOR) pathway, which led to antidepressant-like effects by enhancing synaptogenesis in the medial prefrontal cortex of rodents (Casarotto et al., 2021; Li et al., 2010, 2011). The bidirectional amino acid transport with SLC transporter proteins is known to regulate mTOR activation (Nicklin et al., 2009). Indeed, we found that mTOR was one of the top predicted upstream regulators, which was activated one week after HNK administration. Correspondingly, transporter proteins Slc25a4 and SLC25A5 were also shown to be upregulated one week after HNK administration. Collectively, these results indicate that the activation of the mTOR pathway might play a pivotal mechanistic role in mediating HNK's rapid behavioral effects, comparable to what has been described for ketamine.

It is noteworthy that an extracellular protein, RhoA was associated with the TNF, mTOR and BDNF upstream regulators at 4h following HNK administration. A recent seminal observation by Fox and co-workers has shed light on the role of RhoA in depression by demonstrating that the activation of this protein in the nucleus accumbens contributes to depression-like behavior in the absence of stress (Fox et al., 2018). It is an intriguing finding as RhoA was also found to be up-regulated in the CSF in our study at the 4h time-point after HNK treatment. This phenomenon may be attributed to the secretion of RhoA by the neurons into CSF following HNK treatment, suggesting that HNK reduced the deleterious effects of depression-like phenotype on the neuronal cells by decreasing the expressions of RhoA. A cluster of proteins comprising of MBP, PLP1, GFAP and VIM related to myelin functions, regeneration of neurons and proliferation of neuroglia were also found to be significantly associated with the activation of BDNF, IGF1 and mTOR upstream regulators at 1w treatment of HNK. The protein-protein interaction networks of differentially expressed proteins at both time points (suppl Fig. S3) show the interaction between MBP and PLP1, and our results corroborated with previous finding that demonstrated the association between these proteins using different experimental approaches and both proteins were also shown to form a complex (Arvanitis et al., 2002). Recently, it has been elegantly demonstrated by Martinelli and colleagues that BDNF-modulated neuroplasticity is linked to that activation of GC (Martinelli et al., 2021). It is important to highlight here that BDNF levels are reduced in chronic stress and MDD patients (Martinelli et al., 2021); indicating that the significant regulation of the proteins associated with the activation of BDNF 1w after HNK treatment in our study further strengthens our findings that HNK prevents stress-induced decrease in BDNF levels.

The other top significant canonical pathway affected by HNK vs saline treatment was acute phase response signaling and upstream regulators of TNF and IL6, all of which are closely associated with conditions of enhanced inflammation. Interestingly, we exclusively found this pathway enrichment and the activation of these upstream regulators 1w after HNK administration, but not as early as 4h after injection. As both control animals and HNK-treated animals both underwent the same experimental conditions with surgery and cannula implantation, this induction of inflammatory processes is likely to be a specific effect of HNK. In line with this assumption, recent study by Ho and colleagues showed that both, ketamine and HNK, had a significant impact on inflammation by regulating the STAT3 and Type I Interferon pathway (Ho et al., 2019). Moreover, our mechanistic network analysis demonstrated that most of the proteins involved in mTOR, BDNF and IGF1 pathways are also associated with the TNF and IL6 pathway, namely PLP1, GFAP, VIM and SERPINA1 (Fig. 6C). Further studies on the direct and indirect effects of HNK on inflammatory processes and their contribution to the antidepressant-like effects are needed.

A limitation of this study is that pooled CSF samples were used for the MS-based proteomics analyses. We did not include validation experiments of protein candidates. Although it has been shown that mouse CSF samples can be analyzed individually (Smith et al., 2014), we deliberately chose the pooling paradigm to mitigate inter-individual variations. Moreover, since this is the first study to provide a comprehensive insight into the acute and sustained effects of HNK on murine CSF proteome, it was important to elucidate the overall proteome alterations associated with the use of HNK at the different time-points. Notwithstanding the sample pooling approach, based on the promising results emerging from the current study, the effects of HNK in individual mouse CSF proteome merit further investigation in our next study. Additionally, the alterations observed in the protein markers can be an important yardstick in future translational efforts using human CSF samples in a personalized manner.

In conclusion, our study substantially advances our knowledge about the molecular and cellular mechanisms through which HNK as a prototypical rapid acting antidepressant compound exerts its acute and sustained antidepressant-like effects. We could confirm the DBA/2J inbred mouse strain to be a suitable animal model for investigations into the neurobiological mechanisms underlying rapid-acting antidepressants. Our translationally relevant approach provides unprecedentedly detailed information on the temporal profile of CSF proteome changes in response to HNK. Finally, by a combination of the hypothesis-free mass spectrometry approach with candidate-driven *in vitro* experiments, we identified, for the first time, GR signaling to be a specific target of HNK. We are confident that those data can be a valuable resource for future studies investigating improved, rapid acting strategies to treat depression.

CRediT authorship contribution statement

David P. Herzog: Conceptualization, Methodology, Investigation, Analysis, Funding acquisition, Writing – original draft, Writing – review & editing. **Natarajan Perumal:** Conceptualization, Methodology, Investigation, Analysis, Writing – original draft, Writing – review & editing. **Caroline Manicam:** Methodology, Investigation, Analysis, Writing – original draft, Writing – review & editing. **Giulia Treccani:** Investigation, Analysis, Writing – review & editing. **Jens Nadig:** Investigation, Analysis. **Milena Rossmann:** Investigation, Analysis. **Jan Engelmann:** Investigation, Analysis. **Tanja Jene:** Investigation, Analysis. **Annika Hasch:** Investigation, Analysis. **Michael A. van der Kooij:** Investigation, Analysis. **Klaus Lieb:** Writing – review & editing. **Nils C. Gassen:** Conceptualization, Methodology, Investigation, Analysis, Writing – original draft, Writing – review & editing. **Franz H. Grus:** Conceptualization, Methodology, Analysis. **Marianne B. Müller:** Conceptualization, Methodology, Analysis, Funding acquisition, Writing – original draft, Writing – review & editing.

Declaration of competing interest

Authors declare that they have no conflict of interest.

Acknowledgements

We are thankful for the technical support by Kathrin Kuna (Mainz, Germany). A portion of the work described herein was carried out by Jens Nadig and Milena Rossmann in partial fulfillment of the requirements for a medical doctoral degree at the Johannes Gutenberg University Medical Center Mainz, Germany.

Appendix A. Supplementary data

Supplementary data to this article can be found online at <https://doi.org/10.1016/j.ynstr.2021.100404>.

Funding

DH is supported by the Mainz Research School of Translational Biomedicine (TransMed) with a MD-PhD fellowship. NP is supported by the German Research Foundation (DFG), grant number PE 2531/4-1. CM is supported by the German Research Foundation (DFG), grant number MA 8006/1-1. TJ is supported by the Focus Program of Translational Neurosciences (FTN) in Mainz with a PhD fellowship. GT is supported by a 2014 NARSAD Young Investigator Grant from the Brain & Behavior Research Foundation and the Danish Council for Independent Research, grant number DFF-5053-00103. MM and KL are supported by the German Research Foundation (DFG) within the Collaborative Research Center 1193 (CRC1193, <https://crc1193.de/>) and by the Boehringer Ingelheim Foundation.

Funding sources had no role in study design, data interpretation, and preparation of this paper.

References

- Anacker, C., Zunszain, P.A., et al., 2011. The glucocorticoid receptor: pivot of depression and antidepressant treatment? *Psychoneuroendocrinology* 36 (3), 415–425. <https://doi.org/10.1016/j.psyneuen.2010.03.007>.
- Arango-Lievano, M., Lambert, W.M., et al., 2015. Neurotrophic-priming of glucocorticoid receptor signaling is essential for neuronal plasticity to stress and antidepressant treatment. *Proc. Natl. Acad. Sci. U. S. A.* 112 (51), 15737–15742. <https://doi.org/10.1073/pnas.1509045112>.
- Arvanitis, D.N., Yang, W., Boggs, J.M., 2002. Myelin proteolipid protein, basic protein, the small isoform of myelin-associated glycoprotein, and p42MAPK are associated in the Triton X-100 extract of central nervous system myelin. *J. Neurosci. Res.* 70 (1), 8–23. <https://doi.org/10.1002/jnr.10383>.
- Berman, R.M., Cappiello, A., et al., 2000. Antidepressant effects of ketamine in depressed patients. *Biol. Psychiatr.* 47 (4), 351–354.
- Brachman, R.A., McGowan, J.C., et al., 2016. Ketamine as a prophylactic against stress-induced depressive-like behavior. *Biol. Psychiatr.* 79 (9), 776–786. <https://doi.org/10.1016/j.biopsych.2015.04.022>.
- Browne, C.A., Lucki, I., 2013. Antidepressant effects of ketamine: mechanisms underlying fast-acting novel antidepressants. *Front. Pharmacol.* 4, 161. <https://doi.org/10.3389/fphar.2013.00161>.
- Campagnoni, A.T., Skoff, R.P., 2001. The pathobiology of myelin mutants reveal novel biological functions of the MBP and PLP genes. *Brain Pathol.* 11 (1), 74–91.
- Carrillo-Roa, T., Labermaier, C., et al., 2017. Common genes associated with antidepressant response in mouse and man identify key role of glucocorticoid receptor sensitivity. *PLoS Biol.* 15 (12), e2002690 <https://doi.org/10.1371/journal.pbio.2002690>.
- Casarotto, P.C., Gyrych, M., et al., 2021. Antidepressant drugs act by directly binding to TRKB neurotrophin receptors. *Cell* 184 (5), 1299–1313. <https://doi.org/10.1016/j.cell.2021.01.034> e19.
- Cavalleri, L., Merlo Pich, E., et al., 2018. Ketamine enhances structural plasticity in mouse mesencephalic and human iPSC-derived dopaminergic neurons via AMPAR-driven BDNF and mTOR signaling. *Mol. Psychiatr.* 23 (4), 812–823. <https://doi.org/10.1038/mp.2017.241>.
- Chou, D., Peng, H.Y., et al., 2018. 2R,6R)-hydroxynorketamine rescues chronic stress-induced depression-like behavior through its actions in the midbrain periaqueductal gray. *Neuropharmacology* 139, 1–12. <https://doi.org/10.1016/j.neuropharm.2018.06.033>.
- Cingolani, L.A., Goda, Y., 2008. Actin in action: the interplay between the actin cytoskeleton and synaptic efficacy. *Nat. Rev. Neurosci.* 9 (5), 344–356. <https://doi.org/10.1038/nrn2373>.
- Cox, J., Mann, M., 2008. MaxQuant enables high peptide identification rates, individualized p.p.b.-range mass accuracies and proteome-wide protein quantification. *Nat. Biotechnol.* 26 (12), 1367–1372. <https://doi.org/10.1038/nbt.1511>.
- Cox, J., Neuhauser, N., et al., 2011. Andromeda: a peptide search engine integrated into the MaxQuant environment. *J. Proteome Res.* 10 (4), 1794–1805. <https://doi.org/10.1021/pr101065j>.
- Cox, J., Hein, M.Y., et al., 2014. Accurate proteome-wide label-free quantification by delayed normalization and maximal peptide ratio extraction, termed MaxLFQ. *Mol. Cell. Proteomics* 13 (9), 2513–2526. <https://doi.org/10.1074/mcp.M113.031591>.
- Dong, M., Zeng, L.N., et al., 2019. Prevalence of suicide attempt in individuals with major depressive disorder: a meta-analysis of observational surveys. *Psychol. Med.* 49 (10), 1691–1704. <https://doi.org/10.1017/S0033291718002301>.
- Fitzgerald, P.J., Yen, J.Y., Watson, B.O., 2019. Stress-sensitive antidepressant-like effects of ketamine in the mouse forced swim test. *PLoS One* 14 (4), e0215554. <https://doi.org/10.1371/journal.pone.0215554>.
- Fox, M.E., Chandra, R., et al., 2018. Dendritic remodeling of D1 neurons by RhoA/Rho-kinase mediates depression-like behavior. *Mol. Psychiatr.* <https://doi.org/10.1038/s41380-018-0211-5>.
- Gentsch, C., Lichtsteiner, M., Feer, H., 1981. Locomotor activity, defecation score and corticosterone levels during an openfield exposure: a comparison among individually and group-housed rats, and genetically selected rat lines. *Physiol. Behav.* 27 (1), 183–186.
- Helenius, T.O., Antman, C.A., et al., 2016. Keratins are altered in intestinal disease-related stress responses. *Cells* 5 (3). <https://doi.org/10.3390/cells5030035>.
- Herzog, D.P., Wegener, G., et al., 2019. Decoding the mechanism of action of rapid-acting antidepressant treatment strategies: does gender matter? *Int. J. Mol. Sci.* 20 (4) <https://doi.org/10.3390/ijms20040949>.
- Ho, M.F., Zhang, C., et al., 2019. Ketamine and active ketamine metabolites regulate STAT3 and the type I Interferon pathway in human microglia: molecular mechanisms linked to the antidepressant effects of ketamine. *Front. Pharmacol.* 10, 1302. <https://doi.org/10.3389/fphar.2019.01302>.
- Holsboer, F., 2000. The corticosteroid receptor hypothesis of depression. *Neuropsychopharmacology* 23 (5), 477–501. [https://doi.org/10.1016/S0893-133X\(00\)00159-7](https://doi.org/10.1016/S0893-133X(00)00159-7).
- Johnston, K.M., Powell, L.C., et al., 2019. The burden of treatment-resistant depression: a systematic review of the economic and quality of life literature. *J. Affect. Disord.* 242, 195–210. <https://doi.org/10.1016/j.jad.2018.06.045>.
- Kramer, A., Green, J., et al., 2014. Causal analysis approaches in ingenuity pathway analysis. *Bioinformatics* 30 (4), 523–530. <https://doi.org/10.1093/bioinformatics/bt703>.
- Kretzschmar, A., Schulke, J.P., et al., 2018. The stress-inducible protein DRR1 exerts distinct effects on actin dynamics. *Int. J. Mol. Sci.* 19 (12) <https://doi.org/10.3390/ijms19123993>.
- Labermaier, C., Masana, M., Muller, M.B., 2013. Biomarkers predicting antidepressant treatment response: how can we advance the field? *Dis. Markers* 35 (1), 23–31. <https://doi.org/10.1155/2013/984845>.
- Lener, M.S., Kadriu, B., Zarate Jr., C.A., 2017. Ketamine and beyond: investigations into the potential of glutamatergic agents to treat depression. *Drugs* 77 (4), 381–401. <https://doi.org/10.1007/s40265-017-0702-8>.
- Li, N., Lee, B., et al., 2010. mTOR-dependent synapse formation underlies the rapid antidepressant effects of NMDA antagonists. *Science* 329 (5994), 959–964. <https://doi.org/10.1126/science.1190287>.
- Li, N., Liu, R.J., et al., 2011. Glutamate N-methyl-D-aspartate receptor antagonists reverse behavioral and synaptic deficits caused by chronic stress exposure. *Biol. Psychiatr.* 69 (8), 754–761. <https://doi.org/10.1016/j.biopsych.2010.12.015>.
- Luber, C.A., Cox, J., et al., 2010. Quantitative proteomics reveals subset-specific viral reactivity in dendritic cells. *Immunity* 32 (2), 279–289. <https://doi.org/10.1016/j.immuni.2010.01.013>.
- Lumsden, E.W., Troppoli, T.A., et al., 2019. Antidepressant-relevant concentrations of the ketamine metabolite (2R,6R)-hydroxynorketamine do not block NMDA receptor function. *Proc. Natl. Acad. Sci. U. S. A.* 116 (11), 5160–5169. <https://doi.org/10.1073/pnas.1816071116>.
- Manicam, C., Perumal, N., et al., 2018. Proteomics unravels the regulatory mechanisms in human tears following acute renouncement of contact lens use: a comparison between hard and soft lenses. *Sci. Rep.* 8 (1), 11526 <https://doi.org/10.1038/s41598-018-30032-5>.
- Martinelli, S., Anderzhanova, E.A., et al., 2021. Stress-primed secretory autophagy promotes extracellular BDNF maturation by enhancing MMP9 secretion. *Nat. Commun.* 12 (1), 4643. <https://doi.org/10.1038/s41467-021-24810-5>.
- NICE, 2018. Depression in Adults: Recognition and Management - National Institute for Health and Care Excellence Guidelines [CG90]. National Institute for Health and Care Excellence. www.nice.org.uk/guidance/cg90. (Accessed 29 April 2021).
- Nicklin, P., Bergman, P., et al., 2009. Bidirectional transport of amino acids regulates mTOR and autophagy. *Cell* 136 (3), 521–534. <https://doi.org/10.1016/j.cell.2008.11.044>.
- Olsen, J.V., de Godoy, L.M., et al., 2005. Parts per million mass accuracy on an Orbitrap mass spectrometer via lock mass injection into a C-trap. *Mol. Cell. Proteomics* 4 (12), 2010–2021. <https://doi.org/10.1074/mcp.T500030-MCP200>.
- Onaivi, E.S., Schanz, N., Lin, Z.C., 2014. Psychiatric disturbances regulate the innate immune system in CSF of conscious mice. *Transl. Psychiatry* 4, e367. <https://doi.org/10.1038/tp.2014.5>.
- Perumal, N., Strassburger, L., et al., 2019. Sample preparation for mass-spectrometry-based proteomics analysis of ocular microvessels. *J. Vis. Exp.* 144. <https://doi.org/10.3791/59140>.
- Perumal, N., Strassburger, L., et al., 2020. Bioenergetic shift and actin cytoskeleton remodeling as acute vascular adaptive mechanisms to angiotensin II in murine retina and ophthalmic artery. *Redox Biol.* 101597. <https://doi.org/10.1016/j.redox.2020.101597>.
- Pham, T.H., Defaix, C., et al., 2018. Common neurotransmission recruited in (R,S)-Ketamine and (2R,6R)-hydroxynorketamine-induced sustained antidepressant-like effects. *Biol. Psychiatr.* 84 (1), e3–e6. <https://doi.org/10.1016/j.biopsych.2017.10.020>.
- Rapali, P., Szenes, A., et al., 2011. DYNLL1/LC8: a light chain subunit of the dynein motor complex and beyond. *FEBS J.* 278 (17), 2980–2996. <https://doi.org/10.1111/j.1742-4658.2011.08254.x>.
- Richens, J.L., Spencer, H.L., et al., 2016. Rationalising the role of Keratin 9 as a biomarker for Alzheimer's disease. *Sci. Rep.* 6, 22962 <https://doi.org/10.1038/srep22962>.
- Sathyanesan, M., Girgenti, M.J., et al., 2012. A molecular characterization of the choroid plexus and stress-induced gene regulation. *Transl. Psychiatry* 2, e139. <https://doi.org/10.1038/tp.2012.64>.
- Schulke, J.P., Wochnik, G.M., et al., 2010. Differential impact of tetratricopeptide repeat proteins on the steroid hormone receptors. *PLoS One* 5 (7), e11717. <https://doi.org/10.1371/journal.pone.0011717>.

- Schwartz, J., Murrough, J.W., Iosifescu, D.V., 2016. Ketamine for treatment-resistant depression: recent developments and clinical applications. *Evid. Base Ment. Health* 19 (2), 35–38. <https://doi.org/10.1136/eb-2016-102355>.
- Short, B., Fong, J., et al., 2018. Side-effects associated with ketamine use in depression: a systematic review. *Lancet Psychiatr.* 5 (1), 65–78. [https://doi.org/10.1016/S2215-0366\(17\)30272-9](https://doi.org/10.1016/S2215-0366(17)30272-9).
- Sillaber, I., Panhuysen, M., et al., 2008. Profiling of behavioral changes and hippocampal gene expression in mice chronically treated with the SSRI paroxetine. *Psychopharmacology (Berlin)* 200 (4), 557–572. <https://doi.org/10.1007/s00213-008-1232-6>.
- Smith, J.S., Angel, T.E., et al., 2014. Characterization of individual mouse cerebrospinal fluid proteomes. *Proteomics* 14 (9), 1102–1106. <https://doi.org/10.1002/pmic.201300241>.
- Sobocki, P., Jonsson, B., et al., 2006. Cost of depression in Europe. *J. Ment. Health Pol. Econ.* 9 (2), 87–98.
- Sugimoto, Y., Yamamoto, M., et al., 2011. Differences between mice strains in response to paroxetine in the forced swimming test: involvement of serotonergic or noradrenergic systems. *Eur. J. Pharmacol.* 672 (1–3), 121–125. <https://doi.org/10.1016/j.ejphar.2011.10.002>.
- Thoeringer, C.K., Sillaber, I., et al., 2007. The temporal dynamics of intrahippocampal corticosterone in response to stress-related stimuli with different emotional and physical load: an in vivo microdialysis study in C57BL/6 and DBA/2 inbred mice. *Psychoneuroendocrinology* 32 (6), 746–757. <https://doi.org/10.1016/j.psyneuen.2007.05.005>.
- Toivola, D.M., Boor, P., et al., 2015. Keratins in health and disease. *Curr. Opin. Cell Biol.* 32, 73–81. <https://doi.org/10.1016/j.ceb.2014.12.008>.
- Touma, C., Gassen, N.C., et al., 2011. FK506 binding protein 5 shapes stress responsiveness: modulation of neuroendocrine reactivity and coping behavior. *Biol. Psychiatr.* 70 (10), 928–936. <https://doi.org/10.1016/j.biopsych.2011.07.023>.
- Tyanova, S., Temu, T., Cox, J., 2016. The MaxQuant computational platform for mass spectrometry-based shotgun proteomics. *Nat. Protoc.* 11 (12), 2301–2319. <https://doi.org/10.1038/nprot.2016.136>.
- van der Kooij, M.A., Masana, M., et al., 2016. The stressed cytoskeleton: how actin dynamics can shape stress-related consequences on synaptic plasticity and complex behavior. *Neurosci. Biobehav. Rev.* 62, 69–75. <https://doi.org/10.1016/j.neubiorev.2015.12.001>.
- van der Kooij, M.A., Jene, T., et al., 2018. Chronic social stress-induced hyperglycemia in mice couples individual stress susceptibility to impaired spatial memory. *Proc. Natl. Acad. Sci. U. S. A.* 115 (43), E10187–E10196. <https://doi.org/10.1073/pnas.1804412115>.
- Wang, W., Liu, L., et al., 2019. Ketamine improved depressive-like behaviors via hippocampal glucocorticoid receptor in chronic stress induced-susceptible mice. *Behav. Brain Res.* 364, 75–84. <https://doi.org/10.1016/j.bbr.2019.01.057>.
- Weckmann, K., Deery, M.J., et al., 2019. Ketamine's effects on the glutamatergic and GABAergic systems: a proteomics and metabolomics study in mice. *Mol. Neuropsychiatr.* 5 (1), 42–51. <https://doi.org/10.1159/000493425>.
- Yamaguchi, J.I., Toki, H., et al., 2018. 2R,6R-Hydroxynorketamine is not essential for the antidepressant actions of (R)-ketamine in mice. *Neuropsychopharmacology* 43 (9), 1900–1907. <https://doi.org/10.1038/s41386-018-0084-y>.
- Zanos, P., Moaddel, R., et al., 2016. NMDAR inhibition-independent antidepressant actions of ketamine metabolites. *Nature* 533 (7604), 481–486. <https://doi.org/10.1038/nature17998>.
- Zanos, P., Thompson, S.M., et al., 2018. Convergent mechanisms underlying rapid antidepressant action. *CNS Drugs* 32 (3), 197–227. <https://doi.org/10.1007/s40263-018-0492-x>.